JOURNAL OF VIROLOGY, May 2001, p. 4681–4691 Vol. 75, No. 10
0022-538X/01/$04.00+0 DOI: 10.1128/JVI.75.10.4681–4691.2001

Transport of Human Immunodeficiency Virus Type 1 Pseudoviruses across the Blood-Brain Barrier: Role of Envelope Proteins and Adsorptive Endocytosis

WILLIAM A. BANKS,[1]* ERIC O. FREED,[2] KATHLEEN M. WOLF,[1] SANDRA M. ROBINSON,[1] MARK FRANKO,[1] AND VIJAYA B. KUMAR[1]

GRECC, Veterans Affairs Medical Center—St. Louis, and Division of Geriatrics, Department of Internal Medicine, Saint Louis University School of Medicine, St. Louis, Missouri,[1] and Laboratory of Molecular Microbiology, National Institute of Allergy and Infectious Diseases, National Institutes of Health, Bethesda, Maryland[2]

Received 27 November 2000/Accepted 22 February 2001

Blood-borne human immunodeficiency virus type 1 (HIV-1) crosses the blood-brain barrier (BBB) to induce brain dysfunction. How HIV-1 crosses the BBB is unclear. Most work has focused on the ability of infected immune cells to cross the BBB, with less attention devoted to the study of free virus. Since the HIV-1 coat glycoprotein gp120 can cross the BBB, we postulated that gp120 might be key in determining whether free virus can cross the BBB. We used radioactive virions which do (Env^+) or do not (Env^-) bear the envelope proteins to characterize the ability of HIV-1 to be taken up by the murine BBB. In vivo and in vitro studies showed that the envelope proteins are key to the uptake of free virus and that uptake was enhanced by wheat germ agglutinin, strongly suggesting that the envelope proteins induce viral adsorptive endocytosis and transcytosis in brain endothelia. Capillary depletion showed that Env^+ virus completely crossed the vascular BBB to enter the parenchyma of the brain. Virus also entered the cerebrospinal fluid, suggesting passage across the choroid plexus as well. About 0.22% of the intravenously injected dose was taken up per g of brain. In vitro studies showed that postinternalization membrane cohesion (membrane binding not reversed with acid wash or cell lysis) was a regulated event. Intact virus was recovered from the brain endothelial cytosol and was effluxed from the endothelial cells. These results show that free HIV-1 can cross the BBB by an event related to adsorptive endocytosis and mediated by the envelope proteins.

Human immunodeficiency virus type 1 (HIV-1) produces clinically significant effects on brain function in about 25% of patients with AIDS. These effects range from cognitive impairments to central diabetes insipidus (29, 34). Entry of virus into the central nervous system (CNS) occurs early in the course of HIV-1 infection, predating neurological symptoms and even seroconversion in some patients (1, 59). HIV-1 does not infect neurons and is thought to produce its effects by infecting microglia and astrocytes (1, 3, 64).

To produce these effects on brain, HIV-1 must cross the blood-brain barrier (BBB). Disruption of the BBB is minimal in AIDS (21, 31, 56), and so the virus must negotiate a BBB that is largely intact. Several mechanisms have been suggested for how HIV-1 could cross the BBB (6). One mechanism is that HIV, like togavirus, murine retrovirus, and mumps virus, could first infect the cells which comprise the BBB. HIV-1 has been reported to infect both the brain endothelial cells (1, 3, 55, 64), which comprise the vascular arm of the BBB, and the choroid plexus, which forms the blood-cerebrospinal fluid (CSF) barrier (3, 22). In vitro studies have shown that HIV-1 can infect brain endothelial cells (47–49).

The "Trojan horse" mechanism postulates that infected macrophages cross-activated brain endothelial cells to take up residence in the CNS as infected microglial cells (51, 53). Brain endothelial cells and immune cells activated by cytokines or infection overexpress adhesion molecules and their ligands, promoting the binding of circulating immune cells to brain vasculature (36). Such binding could be the first step in diapedesis, the passage of immune cells across the BBB (44). This close proximity could also facilitate the passage of virus between the infected immune cell and the brain endothelial cell, analogous to the transfer of virus between infected immune cells and epithelial cells (14).

Finally, free virus may also cross the BBB. Fewer data exist on this mechanism, possibly due to the difficulty of studying virus in available models. HIV-1 has been shown in vitro to cross brain endothelial cell monolayers by mechanisms enhanced by tumor necrosis factor alpha and cocaine (16, 69).

The mechanisms by which HIV enters the brain is important. The model for passage of infected immune cells across the BBB has emphasized the CNS as a reservoir of virus for the reinfection of the periphery and mechanisms for neuronal loss and immune cell invasion to explain CNS dysfunction. The ability of cell-free virus to cross the BBB, in contrast, could emphasize the periphery as a continuous source for viral presentation to the CNS. Although free virus that had crossed the BBB would then be available to infect microglia and astrocytes, this model would be more consistent with recent observations suggesting that a large component of neuroAIDS is due to a metabolic encephalopathy that can be reversed when the peripheral viral load is decreased (27).

We have proposed that gp120 could be an important and unifying element for the several mechanisms by which HIV-1 has been suggested to cross the BBB (5). The HIV-1 glyco-

* Corresponding author. Mailing address: VAMC, 915 N. Grand Blvd., St. Louis, MO 63106. Phone: (314) 289-7084. Fax: (314) 289-6374. E-mail: bankswa@slu.edu.

proteins are initially expressed as a polyprotein precursor, gp160, which is cleaved during transport to the cell surface to generate the surface glycoprotein gp120 and the transmembrane glycoprotein gp41. HIV-1 expresses as its viral coat the glycoprotein complex gp160, which is comprised of the integral membrane protein gp41 noncovalently bound to gp120. It is gp120 which binds to the CD4 receptor and coreceptor to initiate membrane fusion and entry into $CD4^+$ cell types (24). In some cells, gp120 binds to galactosylcerimide binding sites (24). However, CD4 and galactosylcerimide are absent from brain endothelial cells (47), and so how gp120 could initiate viral uptake or facilitate the uptake of infected immune cells which express gp120 is not clear. Other glycoproteins, exemplified by wheat germ agglutinin (WGA), can cross the BBB by inducing a vesicular process termed adsorptive endocytosis (15, 61). Adsorptive endocytosis, therefore, provides a classic mechanism by which a glycoprotein like gp120 can interact with the BBB to induce a vesicular pathway for the uptake and transport of virus across the BBB. Adsorptive endocytosis could also be a mechanism for cell to cell transmission of virus, a process dependent on gp120 and stimulated by WGA (19). We have shown gp120 itself crosses the BBB by a process which resembles adsorptive endocytosis, with enhancement of passage by WGA (7, 10, 11). Whether gp120 is important in the uptake by the brain of either free virus or infected immune cells is unclear.

Here we studied the transport across the BBB of radioactively labeled HIV-1 pseudoviruses after intravenous (i.v.) injection into mice. We determined the role of the gp120-gp41 complex by studying viruses which did (Env^+) or did not (Env^-) bear envelope proteins. We also studied in vitro the ability of brain endothelial cells to take up and internalize virus and the ability of the virus to cohere to the membranes of the brain endothelial cell.

MATERIALS AND METHODS

Viral propagation. The plasmid construct for pNL4-3KFS was made by introducing an insertion at the 5′ end of the *env* gene which produced a frameshift, thereby preventing Env protein expression (25). HeLa cell expression produces noninfectious virus particles lacking gp120/gp41 (Env^-). When pNL4-3KFS is cotransfected with the T-cell-tropic Env expression plasmid pIII4-3env (50), the virions produced contained envelope proteins but still lacked a functional *env* gene (Env^+). Virus was separated from cells by centrifugation at $1,000 \times g$ for 30 min, and the virus was then pelleted from this supernatant by ultracentrifugation at $105,000 \times g$ for 2 h.

Radioactive labeling. The Env^+ and Env^- pseudoviruses, recombinant glycoprotein $gp120_{SF}$ (AIDS Reagent Program, Rockville, Md.), and bovine serum albumin (BSA; Sigma Chemical Co., St. Louis, Mo.) were labeled by the chloramine T method (excluding the sodium metabisulfite treatment), a method which can preserve viral infectivity and viral coat protein activity (26, 46). One millicurie of ^{131}I (New England Nuclear, Boston, Mass.), 10 μg of chloramine T, and 5.0 μg of protein (virus or gp120) were incubated together for 60 s. ^{125}I was used to label albumin. The iodinated materials were purified by filtration on G-10 Sephadex (Sigma) columns. Incorporation of the radioactive I, as determined by trichloroacetic acid-brine precipitation, was greater than 90% for all materials, and the specific activities were estimated to be between 50 and 150 Ci/g of protein.

Determination of brain/serum ratios. Male CD-1 mice (Charles River Laboratories, Wilmington, Mass.) weighing 20 to 30 g were anesthetized with an intraperitoneal injection of 40% ethyl carbamate. The left jugular vein and right carotid artery were isolated. A volume of 0.2 ml of 1% BSA in lactated Ringer's solution was injected into the jugular vein. The injection contained 10^6 cpm of $I\text{-}Env^+$ or $I\text{-}Env^-$ virus. Some injections also contained ^{125}I-labeled albumin (I-Alb) or WGA (10 μg/mouse; Sigma). Between 1 and 180 min after injection, blood was obtained from the carotid artery, and the mouse was decapitated. The brain was removed, the pineal and pituitary glands were discarded, and the remainder was weighed; levels of radioactivity were determined in a dual gamma counter that can differentiate ^{125}I and ^{131}I. The whole blood was centrifuged at $5,000 \times g$ for 10 min at 4°C, and the level of radioactivity in the resulting serum was determined. The brain/serum ratio was calculated as (cpm/g of brain)/(cpm/μl of serum).

Measurement of unidirectional influx rate. The permeability of the BBB to virus was measured by determining the blood-to-brain influx rate (K_i, in microliters per gram per minute) by multiple-time regression analysis. To adjust for the clearance of virus and I-Alb from the blood, exposure time (Exp$t$) was calculated from the equation (13, 52) $\text{Exp}t = [\int_0^t \text{Cp}(\tau)d\tau]/\text{Cp}t$, where Cp$t$ is the level of radioactivity in serum at time t and τ is the dummy variable for time. Brain/serum ratios were plotted against Exp$t$, and the regression line for the linear portion of the relation was calculated. The slope of this relation measures K_i, and the intercept measures the distribution volume within brain at $t = 0$ (V_i, in microliters per gram). Lack of a statistically significant relation between the brain/serum ratios and Exp$t$ indicates either that the substance does not cross the BBB or that a steady-state between influx and efflux has already been reached.

Calculation of the percentage of injected material taken up by the brain. The clearance of virus from blood was first characterized. The amount of radioactivity injected i.v. was divided by the level of radioactivity in serum to yield the percentage of injected radioactivity (%Inj) present in 1 ml of serum: %Inj/ml = 100(cpm/ml of serum)/(cpm of injected radioactivity).

To calculate the percentage of the injected dose entering 1 g of brain, the %Inj/ml was divided by 1,000 to convert it to percent injected per microliter. The brain/serum ratios for virus were corrected for vascular contamination by subtracting the brain/serum ratio for albumin (10 μl/g). The resulting brain/serum ratio was then multiplied by percent injected per microliter to yield percent injected per gram.

Capillary depletion. To determine whether virus completely crossed the BBB, we performed capillary depletion with the protocol adapted to mice (30) from rats (60). CD-1 male mice anesthetized with intraperitoneal ethyl carbamate received an i.v. injection of 0.2 ml of lactated Ringer's solution containing 1% BSA, 3×10^6 cpm of virus, and 3×10^6 cpm of I-Alb. Blood from the abdominal aorta was collected, and the cerebral cortex was removed 60 min after i.v. injection. The cerebral cortex was weighed and emulsified with a glass homogenizer (10 strokes) in 0.8 ml of physiological buffer (10 mM HEPES, 141 mM NaCl, 4 mM KCl, 2.8 mM $CaCl_2$, 1 mM $MgSO_4$, 1 mM NaH_2PO_4, 10 mM D-glucose [adjusted to pH 7.4]). Dextran solution (1.6 ml of a 26% solution) was added to the homogenate, which was vortexed and homogenized again (three strokes). Homogenization was performed at 4°C in less than 1 min. An aliquot of the homogenate was centrifuged at $5,400 \times g$ for 15 min at 4°C in a Beckman TL-100 ultracentrifuge with a TLS-55 swinging-bucket rotor. The pellet containing the brain vasculature and the supernatant containing the brain parenchyma were carefully separated. The levels of radioactivity in these fractions and in the aortic serum were determined in a gamma counter. The fractions were expressed as volumes of distribution in microliters per gram, and the parenchymal fraction for virus was corrected for vascular contamination by subtracting the value for the parenchymal fraction for albumin (Pv). The amount of virus retained by brain capillaries (V) was measured by the volume of distribution for the vascular fraction from this experiment.

In another group of mice, the vascular space was washed out to rid the brain of any labeled virus that might be loosely adhering to the luminal side of the capillaries. Sixty minutes after the i.v. injection, the abdominal aorta was severed and arterial blood was collected. The thorax was then opened to expose the heart, both jugular veins were severed, the descending thoracic aorta was clamped, and 20 ml of lactated Ringer's solution injected into the left ventricle of the heart within about 1 min. The cerebral cortex and serum were obtained and processed as described above to obtain parenchyma and brain vasculature fractions. The washed-out parenchyma fraction for virus was corrected by subtracting the parenchyma value for albumin (Pvw). The amount of virus which had crossed the BBB to enter the parenchyma space of the brain was measured by Pvw. The amount of virus reversibly bound by brain vasculature is given by subtracting Pvw from Pv. The total amount of virus exceeding the vascular space of the brain (defined here as the albumin space) is Pv plus V.

Collection of CSF. Each of the mice anesthetized with ethyl carbamate received an i.v. injection of 13×10^6 cpm of $I\text{-}Env^+$ virus and 13×10^6 cpm of I-Alb. Sixty minutes later, the scalp was removed from the posterior aspect of the head, exposing the muscles overlying the posterior fossa. A 30-gauge needle connected to a length of PE-10 tubing was inserted into the posterior fossa with the head in a dependent position. CSF was collected into the PE-10 tubing by capillary action. After collection of about 10 μl of CSF, the tubing was removed, arterial blood was collected from the previously exposed carotid artery, the

mouse was decapitated, and the whole brain was removed. The exact amount of CSF (in microliters) collected was determined by measuring the length (in centimeters) of PE-10 tubing filled with CSF and multiplying by 0.668 (the internal volume of 1 cm of PE-10 tubing is 0.668 μl). Only CSF that was absolutely clear was analyzed. The CSF, brain, and serum were counted in a gamma counter. The results were expressed as brain/serum (microliters per gram), CSF/serum (microliters per milliliter), and brain/CSF (milliliters per gram) ratios.

Isolation of brain microvessels. Murine cerebral microvessels were isolated by a modification of a method of Gerhart et al. (28) All reagent volumes were proportionately adjusted for the quantity of tissue processed; unless otherwise noted, all reagents were of cell culture quality and obtained from Sigma. All glassware and plastics were precoated with phosphate-buffered solution containing 1% BSA to minimize adhesion and to maximize recovery of microvessels. Briefly, 8 to 10 cerebral cortexes from adult male CD-1 mice were pooled and homogenized in cold stock buffer (25 mM HEPES, 1% dextran in minimum essential medium [Gibco BRL, Grand Island, N.Y.] [pH 7.4]) on ice. The homogenate was then filtered through a series of nylon mesh membranes (300-μm pore size, followed by twice through 100-μm pore size; Spectrum, Houston, Tex.), mixed with an equal volume of 40% dextran in stock buffer, and centrifuged at 5,000 × *g* for 15 min at 4°C. The supernatant with a lipid layer was discarded, and the pellet was resuspended in stock buffer and filtered through a 25-μm-pore-size nylon mesh membrane (Bio-Design, Carmel, N.Y.). The microvessels were washed from the surface of the membrane with stock buffer four times, collected, and centrifuged at 5,000 × *g* for 15 min at 4°C. They were resuspended in incubation buffer (129 mM NaCl, 2.5 mM KCl, 7.4 mM Na_2HPO_4, 1.3 mM KH_2PO_4, 0.63 mM $CaCl_2$, 0.74 mM $MgSO_4$, 5.3 mM glucose, 0.1 mM ascorbic acid [pH 7.4]), a small aliquot being reserved for verification of an enriched microvessel preparation by light microscopy. About 97.5% of the cells isolated are capillary endothelial cells, 1.6% are fibroblast-like cells, 0.9% are erythrocytes, and there are no glia, neurons, synaptosomes, or synaptic complexes, although there are some other membrane profiles and myelin fragments (39).

Uptake of virus by IBM. Isolated brain microvessels (IBM) were resuspended in fresh incubation buffer containing 1% BSA (2) to a concentration of about 2.5 mg of capillary protein/ml. Duplicate volumes of 45 μl (100 μg of microvessel protein) were mixed with 11 μl of incubation buffer containing any additives and 4 μl of buffer containing 10^5 cpm of I-Env$^+$ virus (final volume of 60 μl). At time zero (addition of I-Env$^+$ virus), tubes were mixed and incubated at 37°C for 15 min unless otherwise indicated in Results. Microvessels were centrifuged at 10,000 × *g* for 2 min at 4°C in a microcentrifuge, and the supernatants were collected. The pellets were washed with 400 μl of incubation buffer and centrifuged at 10,000 × *g* for 2 min at 4°C; this supernatant was added to the previous one. Both the combined supernatant (S) and the pellet (P) were counted in a gamma counter for 1 min. The percentage of total binding is taken as 100(P)/(S + P).

When measures in addition to percentage of total binding were made, the microvessel pellets resulting from the second incubation buffer wash were subjected to an acid wash procedure in which 400 μl of cold acid wash buffer (0.028 M sodium acetate, 0.12 M NaCl, 0.02 M sodium barbital [pH 3.0]) was added to resuspend the pellets, followed by a 6-min incubation on ice. The tubes were then centrifuged at 10,000 × *g* for 2 min at 4°C, and the supernatants were removed, and the level of radioactivity was determined in a gamma counter. The radioactivity in these tubes was taken to represent binding to the surface of the IBM that was reversible. Acid-washed microvessels were lysed according to the method of Lidinsky and Drewes (41). Acid-washed microvessel pellets were resuspended in 400 μl of distilled water containing 1% BSA and agitated for 2 h at 4°C. They were centrifuged at 15,000 × *g* for 15 min at 4°C, supernatants were removed and saved, and pellets were resuspended and agitated for 1 h at 4°C. After centrifugation at 15,000 × *g* for 15 min at 4°C, the supernatants were pooled with those from the first centrifugation. The level of radioactivity in the pooled supernatants (cytoplasmic fraction [*C*]) and in the pellet (membrane fraction [*M*]) were determined in a gamma counter. Calculations for the various parameters were made as follows: total counts internalized (I) = C + M; total binding (TB) = I + reversible binding (RB); and total counts (TC) added to the tube = TB + S, where S is the combined supernatant of the initial wash as defined above. The parameters submitted to statistical analysis were %TB = 100(TB)/TC; %RB = 100(RB)/TC; %I = 100(I)/TC; and %M = 100(M)/I.

Efflux of virus from IBM. I-Env$^+$ virus and IBM were incubated together at 37°C for 15 min. The mixture was then centrifuged in a microcentrifuge, the supernatants were removed, 400 μl of nonradioactive buffer was added to wash the pellets, and the mixture was centrifuged again. The pelleted cells were resuspended in 400 μl of fresh buffer containing no radioactivity and incubated at 37°C. At 15-min intervals for the next 1 h, these cells were repelleted, the supernatant (efflux supernatants) was collected, and the cells were resuspended in fresh, nonradioactive buffer and incubated at 37°C. The cells were collected after the last efflux supernatant was removed. The level of radioactivity in the cells and efflux supernatants was determined in a gamma counter. The amount of radioactivity available in the cells for efflux at time zero was determined by adding the amounts of radioactivity present in the cells at the end of the study to the total amount of radioactivity effluxed. Results were expressed as the percentage of this number.

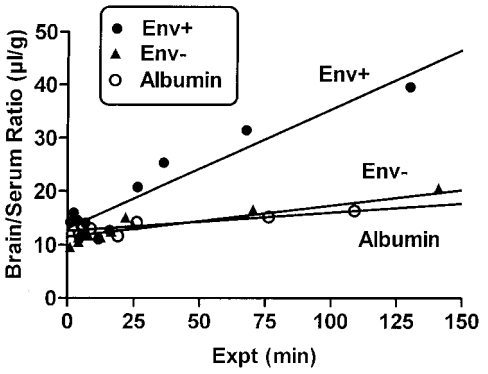

FIG. 1. Transport of Env$^+$ virus, Env$^-$ virus, and albumin across the BBB. The transport of Env$^+$ virus was faster than that of either albumin or Env$^-$ virus. There was no statistically significant difference in the rate of transport of Env$^-$ versus that of albumin.

Identification of radioactive material recovered from biological specimens. The radioactivity in the cell cytoplasm and effluxed by brain endothelial cells was characterized by two methods to determine whether it represented intact virus or shed proteins. The first method was to use a 4B-200 Sepharose column to separate virus, gp120, and smaller proteins based on molecular weight, with higher-molecular-weight substances eluting in earlier fractions. The elution profiles of radioactively labeled virus and gp120 were determined for a 4B-200 Sepharose (Sigma) column by eluting with 100-μl aliquots of 0.25 M phosphate buffer. The elution profile of albumin was determined with methylene blue incubated with a 1% BSA solution in 0.25 M phosphate buffer. Peaks eluted at fractions 8 to 9 for the virus, at fractions 16 to 17 for gp120, and at fractions 21 to 22 for albumin.

The second characterization method was microcentrifugation (65). Radioactivity was placed in 1 ml of a 12% sucrose solution in 0.25 M phosphate buffer, thoroughly mixed, and centrifuged at 20,800 × *g* at 4°C for 2 h. Before and after centrifugation, a 100-μl aliquot was removed and counted. The percentage of material pelleted was determined as [1 − (postcentrifugation cpm/precentrifugation cpm)] × 100. The proportion of material pelleted were 64.4% ± 4.0% for freshly iodinated virus and 16.5% ± 2.2% for freshly labeled gp120.

Statistics. Means are reported with their *n* values and standard error of the mean and compared by analysis of variance. Analyses of groups of more than two means were followed by Duncan's or Newman-Keuls posttest, and the *P* values were reported for relevant statistically significant differences. Regression lines also were calculated by the least squares method with the Prism 3.0 program (GraphPad, Inc., San Diego, Calif.) and are reported with their slopes, intercepts, the error terms (standard deviation of the mean) for the slopes and intercepts, the number of points on which the regression is based (*n*), the correlation coefficient (*r*), and the level of significance for the correlation (*P*). Regression lines were compared for statistical differences with the Prism 3.0 program, which first determines whether there are differences between slopes and, if there are not, whether there are differences between intercepts.

RESULTS

In vivo analyses. Both Env$^+$ and Env$^-$ viruses and albumin had measurable rates of passage from blood to brain, as demonstrated by statistically significant relations between their brain/serum ratios and Exp*t* (I-Env$^+$ virus, $n = 10$, $r = 0.951$, $P < 0.0001$; I-Env$^-$ virus, $n = 12$, $r = 0.958$, $P < 0.0001$; I-Alb, $n = 8$, $r = 0.850$, $P < 0.01$) (Fig. 1). The rate of passage as

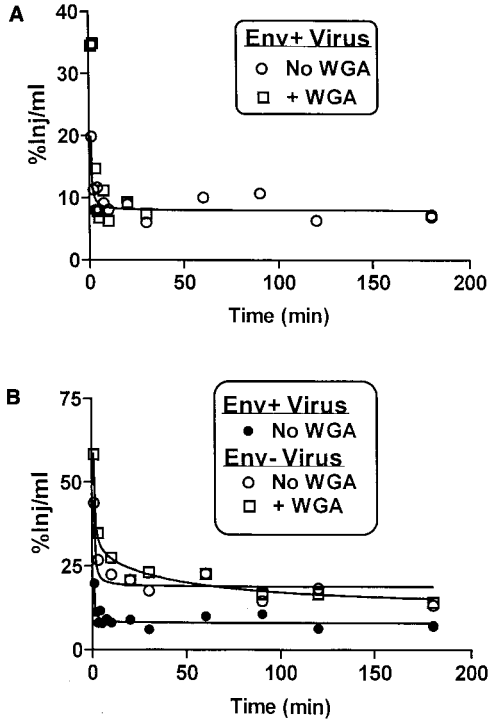

FIG. 2. Clearance of virus from blood after i.v. injection. (A) Clearance of Env$^+$ virus. WGA had little effect on clearance. (B) Clearance of Env$^-$ virus. WGA had little effect on clearance. Env$^+$ (no WGA) is shown for reference.

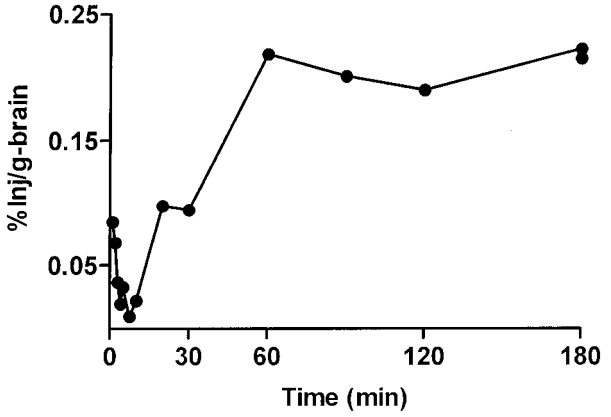

FIG. 3. Percentage of an i.v. dose of Env$^+$ virus taken up per gram of brain. Results have been corrected for the vascular space of the brain. Peak value was about 0.22%/g.

measured by the unidirectional influx rate (K_i) for Env$^+$ virus was 0.228 ± 0.026 μl/g/min. This was over five times greater than the K_i for I-Alb of 0.034 ± 0.008 μl/g/min and was statistically different from it: $F(1,14) = 38.9$, $P < 0.0001$. The Ki for Env$^-$ virus was 0.058 ± 0.005 μl/g/min and was statistically different from the K_i for I-Env$^+$ virus [$F(1,19) = 59.5$, $P < 0.001$] but not for I-Alb.

Viral clearance from blood followed a two-phase distribution pattern (Fig. 2). An early distribution phase occurred for the earliest time points (3 min or less), after which a plateau phase was reached. For Env$^+$ virus, this plateau gave a value of about 8% Inj/ml (Fig. 2A), or a volume of distribution of about 12.5 ml. For Env$^-$ virus, the plateau was about 20% (Fig. 2B), giving a volume of distribution of 5 ml, or a little over twice the vascular space of the mouse. Injection of WGA did not affect viral clearance except to increase the earliest time point.

The level of injected Env$^+$ virus in the brain peaked at about 0.22%/g of brain (Fig. 3). The peak occurred 60 min after injection and remained stable for 180 min after i.v. injection.

WGA acutely increased the uptake of Env$^+$ virus but had no effect on Env$^-$ virus (Fig. 4), consistent with a role for adsorptive endocytosis in viral uptake. Figure 4A shows a pilot study which indicated that WGA produced an immediate, short-term increase in the uptake of Env$^+$ virus as previously seen for gp120. WGA had no statistically significant effect on Env$^-$ virus. Values below zero show when brain/serum ratios for virus were lower than those for coinjected I-Alb. Figure 4B shows results for mice that received an i.v. injection containing I-Env$^+$ or I-Env$^-$ virus and I-Alb with or without WGA. Brain and serum were collected 5 min after i.v. injection, and the brain/serum ratios for virus were corrected for vascular space as measured with I-Alb. The results show that WGA had an effect on I-Env$^+$ virus uptake: $F(3,16) = 11.29$, $P < 0.0005$, $n = 5$/group, increasing uptake about 15 times. The range test showed that the I-Env$^+$ virus-plus-WGA group differed from the groups of I-Env$^+$ virus ($P < 0.01$), I-Env$^-$ virus plus WGA ($P < 0.01$), and I-Env$^-$ virus ($P < 0.001$). WGA had no effect on Env$^-$ virus uptake; the negative values suggest that Env$^-$

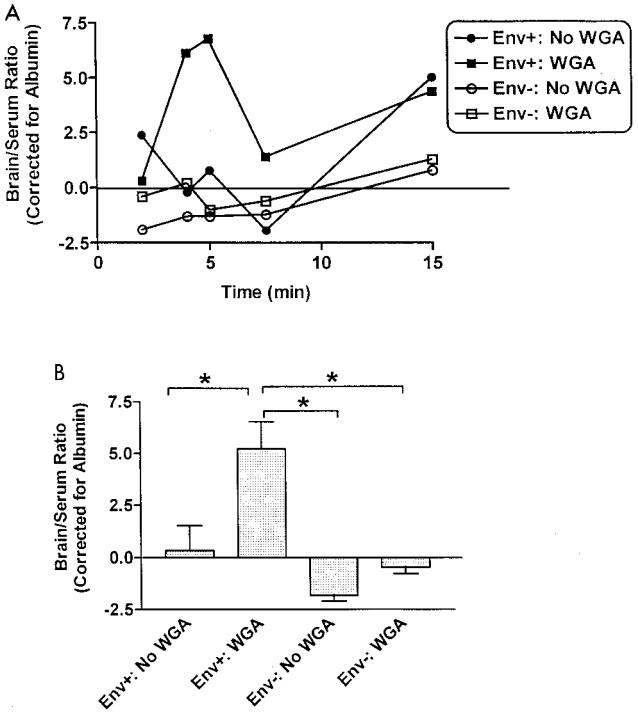

FIG. 4. Effect of WGA on virus uptake. (A) Pilot study showing that WGA had an effect on Env$^+$ virus uptake but not on Env$^-$ virus uptake; (B) effect of WGA on the uptake of Env$^+$ and Env$^-$ virus 5 min after i.v. injection. WGA produced a statistically significant enhancement of Env$^+$ uptake but not of Env$^-$ uptake.

TABLE 1. Distribution of extravascular I-Env$^+$ virus as determined by capillary depletion.

Compartment[a]	Ratios (μl/g)	% Extravascular
Total extravascular	8.70 ± 0.90	100 ± 11.3
Parenchyma	7.23 ± 0.51	83.1 ± 5.8
Capillary (total)	1.55 ± 0.42	17.8 ± 4.8
Reversible	0.85 ± 0.48	9.8 ± 5.5
Internalized	0.70 ± 0.04	8.0 ± 0.5

[a] n = 5/group. Total extravascular measures the amount of I-Env$^+$ virus in cortical tissue not accounted for by the albumin (vascular) space; it comprises parenchymal and capillary (total). Reversible and internalized are subcompartments of capillary (total).

virus distributes into a slightly smaller vascular space in the brain than does serum albumin. No other differences occurred among these groups. This shows that WGA-enhanced adsorptive endocytosis is dependent on the presence of gp120 and gp41 envelope proteins in HIV-1.

Capillary depletion was used to determine whether the I-Env$^+$ taken up by the brain completely crossed the BBB or was sequestered by the capillary bed. The results showed that the majority of I-Env$^+$ virus crossed the BBB completely to enter the brain parenchymal space (Table 1). Smaller amounts of I-Env$^+$ virus (less than 1 μl/g) were reversibly bound to capillaries or were retained by capillaries.

CSF was collected to determine whether i.v.-injected Env$^+$ could enter this compartment of the CNS. The entry of I-Env$^+$ virus into CSF exceeded that of I-Alb, as shown by the CSF/serum ratios (Fig. 5A); the brain/serum ratios for I-Env$^+$ virus and I-Alb are also shown for comparison. The I-Alb value for brain/serum ratios represents primarily the vascular space of the brain. Properly collected CSF has no vascular component, and the albumin value for CSF/serum ratios primarily represents residual leakage of the BBB through extracellular pathways (4). Correction of brain/serum and CSF/serum ratios for I-Env$^+$ virus by subtracting the I-Alb ratios yields more specific measures of viral uptake, even though I-Alb is correcting brain and CSF for different nonspecific measures. Figure 5B shows that the CSF/serum and brain/serum ratios corrected for the albumin spaces exceed zero, demonstrating that virus enters both compartments. The brain/CSF ratio exceeded unity, suggesting that the choroid plexus is less permeable to I-Env$^+$ virus than is the vascular barrier.

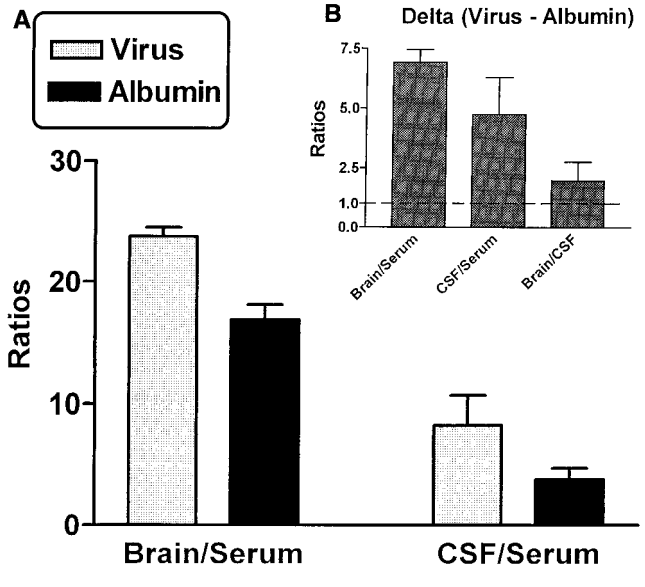

FIG. 5. Viral entry into CSF compartment after i.v. injection of Env$^+$. (A) Comparison of brain/serum and CSF/serum ratios; (B) ratios corrected for albumin space. The dashed line represents unity and shows that the albumin-corrected brain/CSF ratio is greater than 1.

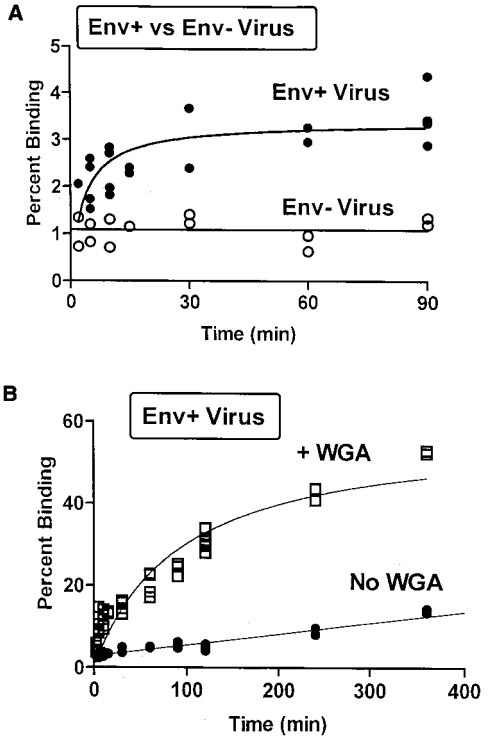

FIG. 6. Percentage of total binding by IBM. (A) Comparison of capillary binding of Env$^+$ and Env$^-$ virus (No WGA); (B) comparison of uptake of Env$^+$ virus incubated with or without WGA.

In vitro analyses. In vitro incubation of IBM with I-Env$^+$ virus showed that brain microvessels took up virus in a time-dependent manner. Figure 6A compares I-Env$^+$ virus uptake to I-Env$^-$ virus uptake for the first 90 min of incubation. The percent binding of I-Env$^-$ virus averaged 1.09% ± 0.8% and did not increase over time. The highest value for I-Env$^-$ virus was lower than the lowest value for I-Env$^+$ virus. This shows that Env proteins are crucial to the specific uptake of HIV-1 by the brain endothelial cells which comprise the BBB. Uptake of I-Env$^+$ virus was rapid for about 15 min (Fig. 6A) and then entered a more steady uptake phase which lasted at least 6 h (Fig. 6B). WGA (50 μg/ml) increased greatly (three to fivefold at most time points) the uptake of I-Env$^+$ virus by IBM.

We determined the fate of Env$^+$ virus taken up by IBM. When cells were incubated for 2 h with I-Env$^+$ virus, WGA increased the percentages of total binding, internalization, and reversible binding (Fig. 7A to C, respectively) of Env$^+$ virus in a dose-response manner (n = 5/concentration). This shows that the majority of Env$^+$ taken up by IBM is internalized and very little is loosely bound to the surface. These results also

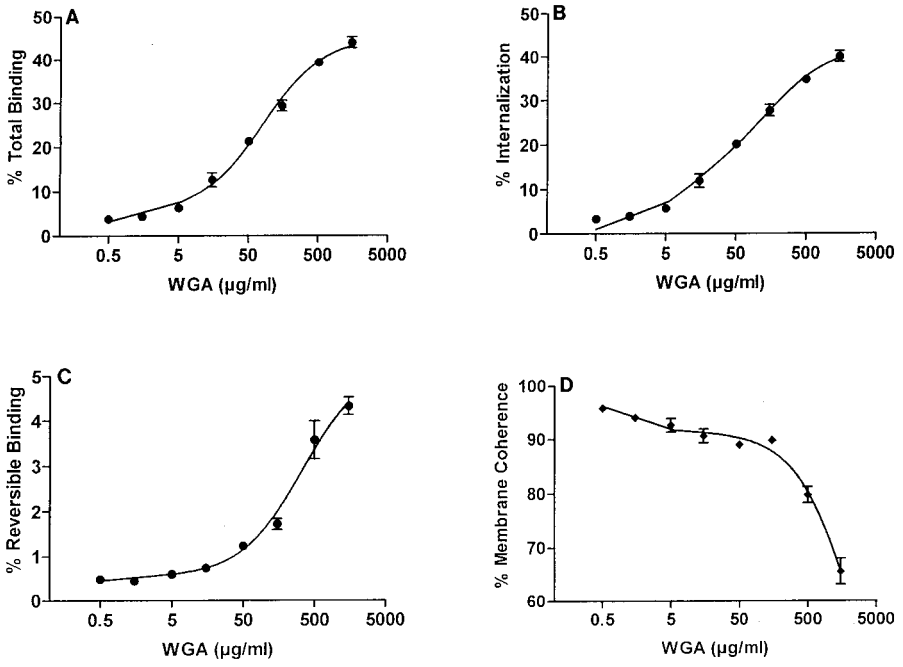

FIG. 7. Fate of Env$^+$ virus taken up by IBM. For details of measurements, see Materials and Methods.

demonstrate that WGA promotes this internalization. The percentage of internalized Env$^+$ virus that cohered to membranes decreased in a dose-response manner (Fig. 7E) from 95.8 ± 0.5 with no WGA to 65.6 ± 2.4 at 1,500 μg of WGA per ml. This shows the majority of internalized virus is strongly integrated with, and perhaps fused to, the membrane compartment. The decrease in percentage of membrane coherence percent internalization increases shows both that internalization and membrane cohesion are separate processes and suggest that factors promoting the former are limited. Alternatively, WGA could inhibit membrane cohesion. The Prism software program determined that the two-site model was a better fit than the one-site model for the results shown in Fig. 7.

To determine whether increasing WGA could decrease percentage of membrane coherence at short incubation times, an abbreviated dose-response curve was performed at a 15-min incubation period. WGA once again increased percentages of total binding, internalization, and reversible binding (Fig. 8A to C, respectively) in a dose-response manner (n = 5/concentration). Values for membrane coherence (Fig. 8D) were similar to those in Fig. 7D, decreasing from 91.3% ± 0.3% with no WGA to 65.3% ± 0.8% at 1,500 μg/ml of WGA.

Protamine sulfate (PS) is a polycation that can induce adsorptive endocytosis in brain endothelial cells (62, 63) and reverse gp120 membrane coherence (7). We determined whether PS at 1 mg/ml, an optimal dose for promoting gp120 membrane coherence (7), could affect the uptake, internalization, and membrane coherence of Env$^+$ virus by IBM. The results for the effect of PS on percentages of total binding [$F(3,8) = 580$, $P < 0.001$), internalization [$F(3,8) = 197$, $P < 0.001$), reversible binding [$F(3,8) = 6.77$, $P < 0.05$), and membrane coherence [$F(3,8) = 29.3$, $P < 0.001$) are shown in Fig. 9 (n = 3/group). The posttest showed that PS (1 mg/ml), WGA (50 μg/ml), and PS plus WGA increased percentages of total binding, internalization, and reversible binding all at $P < 0.05$ or less. PS increased percentages of total binding and internalization more than WGA ($P < 0.001$), and PS plus WGA increased these values more than PS or WGA alone ($P < 0.001$). PS plus WGA also increased percentage reversible binding more than PS or WGA alone ($P < 0.01$). These results show that both WGA and PS alone or together promote viral binding and internalization by IBM. WGA and PS plus WGA decreased the percentage of membrane coherence ($P < 0.01$), but PS alone did not. This value was decreased more by PS plus WGA than by WGA alone ($P < 0.01$), again showing that WGA affects percentages of internalization and membrane coherence differently.

To determine whether the radioactivity internalized by IBM represented intact virus, we lysed the cells and submitted the resulting cytoplasm to Sepharose column chromatography. The radioactivity was derived from IBM incubated with Env$^+$ virus and PS plus WGA to retard membrane coherence. The results (Fig. 10A) showed that 50.6% of the radioactivity eluted in the position of virus at fractions 7 to 10. Cytosolic radioactivity was also submitted to sucrose centrifugation; 32.1% less radioactivity was found in the postcentrifugation phase. This shows intact virus can reside inside brain endothelial cells and should be available for either infecting the cell or being effluxed to the luminal or abluminal surface.

To determine whether intact virus is effluxed from IBM, we preincubated Env$^+$ virus with IBM, washed and transferred the IBM to nonradioactive media, and collected and characterized the effluxed radioactivity. Efflux was greatest during the first 15 min (Table 2). About 25% of the radioactivity effluxed during the first 15 min eluted on Sepharose as intact virus, with other peaks eluting in the region of I-gp 120 and of smaller

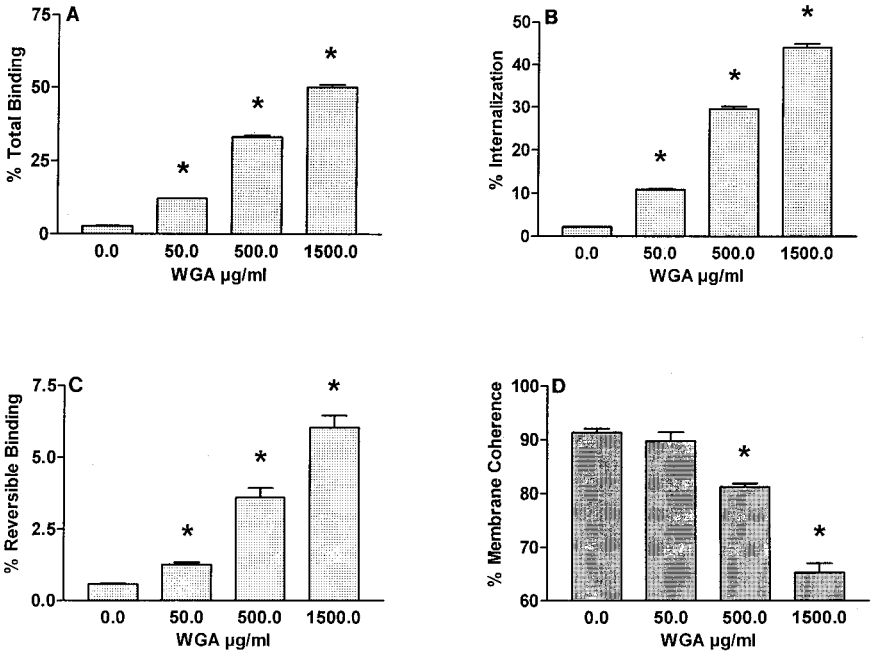

FIG. 8. Effect of WGA on fate of Env^+ taken up by IBM. WGA increased percentages of total binding, reversible binding, and internalization in a dose-response manner. The percentage of membrane coherence decreased with increasing WGA concentration. *, $P < 0.05$ in comparison to no dose.

proteins (Fig. 10B). About 96.4% of effluxed radioactivity could be precipitated by acid. This shows that brain endothelial cells can discharge intact virus and viral proteins into their environment.

DISCUSSION

The purpose of these studies was to characterize the ability of HIV-1 to cross the BBB as free virus. The use of pseudotyped virions has distinct advantages for this purpose. By constructing virions with (Env^+) and without (Env^-) envelope proteins, we were able to test the hypothesis that gp120/gp41 is key to viral uptake by the BBB. The virions, even those with envelope proteins, do not carry the *env* gene and so do not produce infectious virions. This allows us to study events related to the uptake of an initial, exogenously administered viral load. These results, therefore, most closely reflect events during the early stage of HIV-1 invasion into the CNS before astrocytes and glial cells become infected. Major findings for this study are: (i) the Env proteins are necessary for the transport of i.v.-injected HIV-1 virions across the BBB; (ii) transport characteristics of Env^+ virus resemble adsorptive endocytosis, including enhancement by WGA; (iii) virus likely enters the CNS at both the vascular BBB and the choroid plexus; (iv) the majority of virus taken up from the circulation completely crosses the BBB to enter the parenchymal and CSF compartments of the brain; (v) in vitro studies confirm the major in vivo findings, including the importance of Env proteins and adsorptive endocytosis-like mechanisms of uptake; (vi) Binding, internalization, postinternalization membrane cohesion, and efflux are identifiable phases in the uptake of Env^+ virions by brain endothelial cells; and (vii) a portion of the virus taken up by brain endothelial cells resides intact in and is effluxed intact from brain endothelial cells. Taken together, these findings show that blood-borne HIV-1 is capable of crossing the BBB. The results supporting each of these findings are discussed below.

The Env^+ virus was taken up by the brain after i.v. injection into the mouse about seven times faster than albumin even though the virus is much larger than albumin. This shows that uptake of virus was not due to leakage or entry of virus through the extracellular pathways but involves mechanisms for selective permeability. Since the albumin and virus were coinjected, the possibility that virus induced a disruption of the BBB is ruled out, as the uptake of the smaller albumin molecule would have been at least as great as that of virus. The uptake of Env^- virus was not statistically different from the uptake of albumin. This marked difference between the uptake rates of Env^- and Env^+ viruses shows the importance of envelope proteins in the uptake of free virus by the BBB. This role for envelope proteins in the uptake of free virus differs from the mechanisms proposed for the transport across the BBB of infected immune cells, which has emphasized the interaction of adhesion molecules and ligands (44). A role for the envelope proteins in viral uptake is consistent with work by others. For example, virus-sized latex particles covalently coated with gp120 are taken up by epithelial cells (38), the C1 region of gp120 determines endothelial tropism independently of macrophage or T-cell tropism (49), and the CD4-independent uptake of HIV-1 by HeLa cells is gp120 dependent (45). The presence of envelope proteins also increased the volume of distribution after i.v. injection two- to threefold (Fig. 2), consistent with gp120/gp41 being important for the uptake of HIV-1 by non-CNS tissues.

The percentage of Env^+ virus taken up by the brain after i.v.

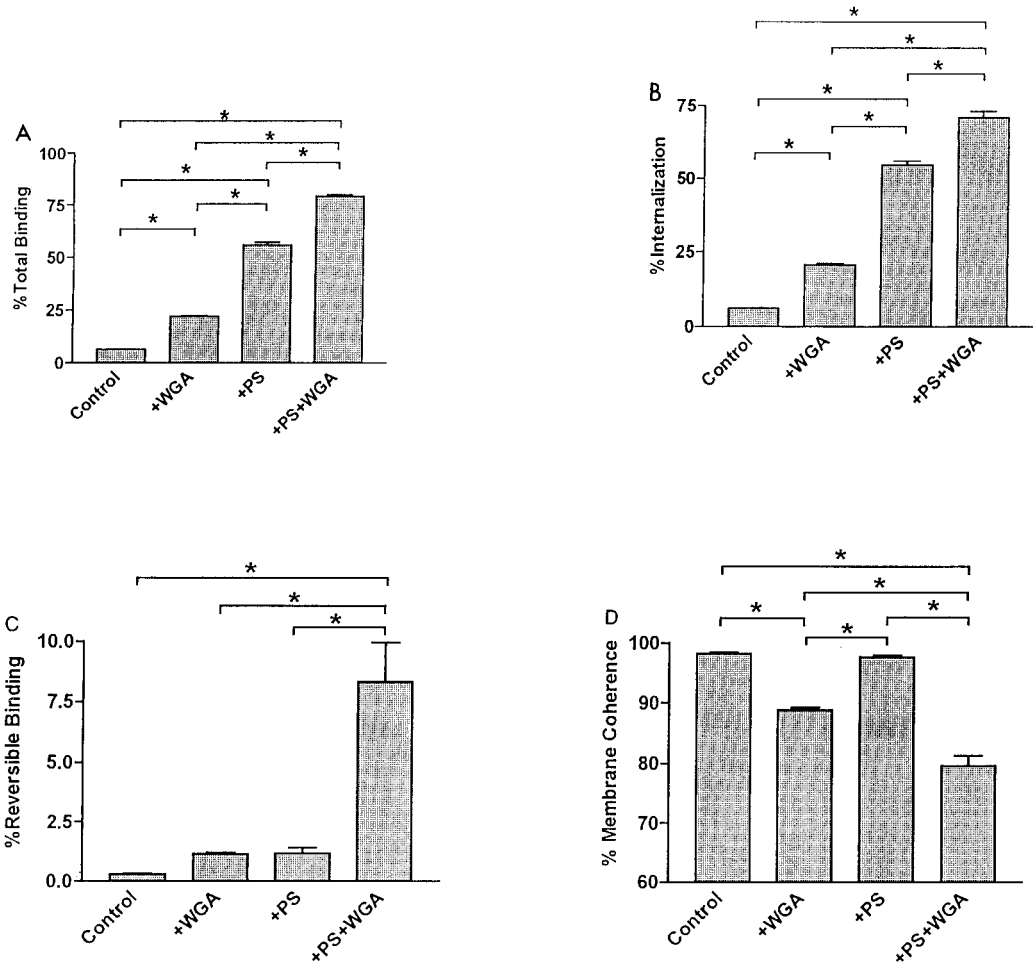

FIG. 9. Effects of WGA, PS, and PS plus WGA on fate of Env^+ virus taken up by IBM. WGA, PS, and PS plus WGA increased percentage of total binding and internalization; the percentage of reversible binding was increased only with PS plus WGA. WGA and PS plus WGA but not PS alone decreased the percentage of membrane coherence. *, $P < 0.05$ for indicated comparisons.

injection was 0.22/g of brain, a value higher than those for some centrally active substances such as morphine (0.018%), leptin (0.17%), biphalan (0.05%), or domoic acid (0.002%) (9, 12, 35, 57). Uptake was also sustained, continuing for at least 3 h. This shows that a sizable percentage of virus can enter and be retained by the brain.

WGA induced an acute, 15-fold increase in the uptake of Env^+ virus but had no effect on the uptake of the Env^- virus. This shows the WGA interaction was dependent on the presence of envelope proteins and is consistent with the adsorptive endocytosis hypothesis for HIV-1 uptake. The magnitude of the WGA-induced increase in the uptake of Env^+ virus was similar to the 17-fold increase previously seen for free gp120 (10, 11). The ability of WGA to induce uptake of Env^+ virus suggests that the gp120 portion of the gp120/gp41 complex binds to the same sugars on the endothelial cell as WGA (sialic acid and *N*-acetylglucosamine). This is consistent with previous work with gp120, which shows that lectins which bind to sugars other than sialic acid and *N*-acetylglucosamine do not promote the transport of gp120 across the BBB (10). When WGA binds to sialic acid and *N*-acetylglucosamine, it induces vesicle-mediated internalization of WGA by brain endothelial cells, termed adsorptive endocytosis (8, 17). Lectin-induced vesicles provide the basis by which enveloped viruses in general are internalized by cells (43). Together, these results strongly suggest that gp120 or gp120/gp41 induces adsorptive endocytosis and the uptake of HIV-1 by brain endothelial cells. Such uptake would provide a mechanism by which brain endothelial cells could become infected with free, blood-borne virus.

Infected brain endothelial cells could infect the brain by shedding virus from their abluminal surface into the brain interstitial fluid. Others have suggested that replication in endothelial cells is less important than direct viral transfer across the BBB (55). The results for capillary depletion show that Env^+ virus taken up from blood is able to completely cross the BBB. In fact, very little Env^+ virus was retained by brain endothelial cells; most was found in the brain parenchymal fraction. These results are similar to those previously found for free gp120. In most cases, the material taken up by adsorptive endocytotic pathways is effluxed back to the luminal surface of the brain endothelial cell (18, 58, 61). Other pathways route the vesicles to lysosomes, the Golgi complex, and eventually

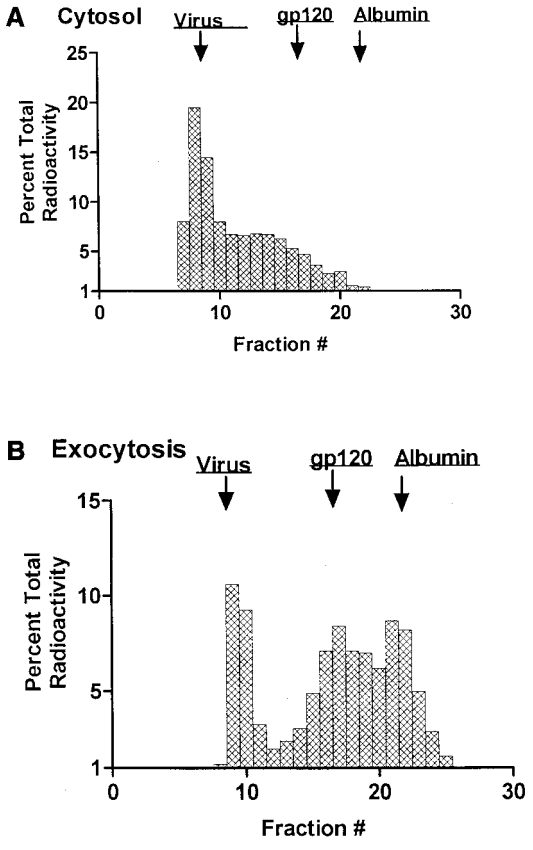

FIG. 10. Identification of radioactivity recovered from IBM. Radioactivity was characterized on a 4B-200 Sepharose column. The elution peaks for virus, gp120, and albumin as determined for this type of column are shown. (A) Characterization of radioactivity recovered from the cytoplasm of IBM that had been incubated with Env^+ virus. Over 50% eluted in the position of virus. (B) Characterization of radioactivity effluxed by IBM that had been preincubated with Env^+ virus. About 25% of effluxed material eluted in the position of virus, showing that intact virus survives endocytosis and exocytosis to either the luminal or abluminal surface.

the abluminal surface of the endothelial cell. HIV-1 has a major advantage in some of these pathways in that it is not degraded in lysosomes (14). This work shows that at least some of the pathways for endocytosed HIV-1 are transcytotic.

The appearance of Env^+ virus in the CSF also demonstrates that HIV-1 can enter a compartment of the CNS from the circulation. Whether virus in the CSF entered the CNS at the vascular barrier with diffusion through the interstitial fluid to CSF or crossed at the choroid plexus is unclear. The choroid plexus does take up HIV-1 (3, 22, 33) and is a vesicularly active tissue (37). In contrast, material transported into the CSF does not penetrate deeply into brain tissue (42). Brain/serum ratios, therefore, tend to reflect passage at the vascular barrier, whereas CSF/serum ratios tend to reflect passage at the choroid plexus, especially at early time points. The brain/CSF ratio of greater than unity has been suggested to indicate that the vascular barrier is the major site of entry. Most likely, HIV-1 crosses at both the vascular barrier and the choroid plexus.

TABLE 2. Efflux of radioactivity from brain endothelial cells preloaded with I-Env^+ virus[a]

Time (min)	% Efflux	
	15 min	Cumulative
0–15	12.2 ± 0.6	12.2 ± 0.6
15–30	4.7 ± 0.3	16.9 ± 0.4
30–45	3.2 ± 0.2	20.1 ± 0.3
45–60	2.6 ± 0.3	22.6 ± 0.3

[a] n = 3/group. Brain endothelial cells were preloaded by incubating them for 15 min with I-Env^+ virus.

The results with isolated brain microvessels confirmed and extended the in vivo findings. Env^+ virus uptake was time dependent and enhanced by WGA. In contrast, the uptake of Env^- virus was low, did not increase with time, and was not enhanced by WGA. As with gp120 uptake by IBM, the uptake of Env^+ virus could be divided into reversible binding, internalization, and membrane coherence. With this method, the fate of material not effluxed to the luminal or abluminal surfaces can be followed. Consistent with models of adsorptive endocytosis, most of the material taken up was internalized (as opposed to reversible cell surface binding). In addition, almost all of the internalized material cohered to the membrane fraction after lysis of the cells (membrane coherence). Such coherence shows a strong association with the membranes that is likely irreversible. Similar membrane coherence has been shown for gp120 and is due to binding to the cell cytoskeleton (7). Whether this membrane coherence represents viral fusion to the membrane is not clear. The percentage of internalized material showing postlysis membrane coherence decreased as internalization increased. This suggests that the intracellular substrates which mediate membrane coherence are limited relative to those which mediate internalization, which in turn suggests that this pathway could become overwhelmed with high viral titers in blood, which would shift more virus into the efflux and transcytotic routes. When these experiments were repeated after a 15-min incubation rather than 2 h, the results were nearly identical. This indicates that consumption of the rate-limiting membrane cohesion factor occurs rapidly. Consistent with this possibility, about 25% of the radioactivity effluxed from IBM eluted as free virus and the rest eluted as large proteins.

PS also can induce vesicularization of brain endothelial cells as do many other highly charged cations (32, 62, 63). PS also increased binding and internalization of Env^+ virus. At the concentrations tested, PS was more potent than WGA in inducing internalization but less potent at inhibiting membrane coherence. This demonstrates that binding and membrane coherence are separate processes, as previously suggested from work based on gp120 (7). Consistent with this decrease in membrane coherence, about half of the radioactivity recovered from the cytosol of these cells eluted as intact virus.

The ability of HIV-1 to interact with murine endothelial cells raises questions of species specificity. HIV-1 most readily infects $CD4^+$ primate immune cells. This species and tissue specificity is reinforced by blocks involving membrane fusion and Tat and Rev function (54, 66). However, neither species nor tissue specificity is absolute, with some strains of HIV-1 better at overcoming the blocks than others (54). Furthermore, rabbits can become infected with HIV-1 (23) and some types of CD4-negative cells (23, 40), and lines of rodent cells can sup-

port HIV-1 infection (54). Human brain endothelial cells take up HIV-1 by a CD4-independent mechanism. We have postulated that interactions between viral and cell surface glycoproteins induce adsorptive endocytosis in brain endothelial cells, a classic response which provides a mechanism for the uptake and passage of HIV-1 across the BBB. Specificity is determined by the sugars presented on the glycoproteins. The distribution of sialic acid and *N*-acetylglucosamine, the sugars to which WGA and possibly HIV-1 envelope proteins bind, show cell type and cell surface distribution specificity but are present on mouse, rat, and human brain endothelial cells (8, 20, 67, 68) and could explain how murine brain endothelial cells can readily take up a pathogen ordinarily so restricted to infecting humans.

In conclusion, in vivo and in vitro studies show that free HIV-1 can be taken up by brain endothelial cells and cross the BBB. The envelope proteins are critical to this process, in that they appear to induce adsorptive endocytosis and transcytosis.

ACKNOWLEDGMENTS

This work was supported by VA Merit Review, R0-1 MH54979, and R0-1 NS41863.

REFERENCES

1. **An, S. F., M. Groves, F. Gray, and F. Scaravilli.** 1999. Early entry and widespread cellular involvement of HIV-1 DNA in brains of HIV-1 positive asymptomatic individuals. J. Neuropathol. Exp. Neurol. **58:**1156–1162.
2. **Audus, K. L., and R. T. Borchardt.** 1987. Bovine brain microvessel endothelial cell monolayers as a model system for the blood-brain barrier. Ann. N. Y. Acad. Sci. **507:**9–18.
3. **Bagasra, O., E. Lavi, L. Bobroski, K. Khalili, J. P. Pestaner, R. Tawadros, and R. J. Pomerantz.** 1996. Cellular reservoirs of HIV-1 in the central nervous system of infected individuals: indentification by the combination of in situ polymerase chain reaction and immunohistochemistry. AIDS **10:**573–585.
4. **Balin, B. J., R. D. Broadwell, M. Salcman, and M. el-Kalliny.** 1986. Avenues for entry of peripherally administered protein to the central nervous system in mouse, rat, and squirrel monkey. J. Comp. Neurol. **251:**260–280.
5. **Banks, W. A.** 1999. Physiology and pathophysiology of the blood-brain barrier: implications for microbial pathogenesis, drug delivery and neurodegenerative disorders. J. Neurovirology **5:**538–555.
6. **Banks, W. A.** 2000. Protector, prey, or perpetrator: the pathophysiology of the blood-brain barrier in neuroAIDS. NeuroAIDS **3:**1–6. [Science Online.] www.sciencemag.org/NAIDS.
7. **Banks, W. A., V. Akerstrom, and A. J. Kastin.** 1998. Adsorptive endocytosis mediates the passage of HIV-1 across the blood-brain barrier: evidence for a post-internalization coreceptor. J. Cell Sci. **111:**533–540.
8. **Banks, W. A., and R. D. Broadwell.** 1994. Blood to brain and brain to blood passage of native horseradish peroxidase, wheat germ agglutinin and albumin: pharmacokinetic and morphological assessments. J. Neurochem. **62:**2404–2419.
9. **Banks, W. A., and A. J. Kastin.** 1994. Opposite direction of transport across the blood-brain barrier for Tyr-MIF-1 and MIF-1: comparison with morphine. Peptides **15:**23–29.
10. **Banks, W. A., and A. J. Kastin.** 1998. Characterization of lectin-mediated brain uptake of HIV-1 gp120. J. Neurosci. Res. **54:**522–529.
11. **Banks, W. A., A. J. Kastin, and V. Akerstrom.** 1997. HIV-1 protein gp120 crosses the blood-brain barrier: role of adsorptive endocytosis. Life Sci. **61:**PL119–PL125.
12. **Banks, W. A., A. J. Kastin, W. Huang, J. B. Jaspan, and L. M. Maness.** 1996. Leptin enters the brain by a saturable system independent of insulin. Peptides **17:**305–311.
13. **Blasberg, R. G., J. D. Fenstermacher, and C. S. Patlak.** 1983. Transport of α-aminoisobutyric acid across brain capillary and cellular membranes. J. Cereb. Blood Flow Metab. **3:**8–32.
14. **Bourinbaiar, A. S., and D. M. Phillips.** 1991. Transmission of human immunodeficiency virus from monocytes to epithelia. J. Acquir. Immune Defic. Syndr. **4:**56–63.
15. **Broadwell, R. D.** 1989. Transcytosis of macromolecules through the blood-brain barrier: a cell biological perspective and critical appraisal. Acta Neuropathol. (Berlin) **79:**117–128.
16. **Broadwell, R. D.** 1993. Endothelial cell biology and the enigma of transcytosis through the blood-brain barrier. Adv. Exp. Med. Biol. **331:**137–141.
17. **Broadwell, R. D., B. J. Balin, and M. Salcman.** 1988. Transcytotic pathway for blood-borne protein through the blood-brain barrier. Proc. Natl. Acad. Sci. USA **85:**632–636.
18. **Broadwell, R. D., and W. A. Banks.** 1993. Cell biological perspective for the transcytosis of peptides and proteins through the mammalian blood-brain fluid barriers, p. 165–199. *In* W. M. Pardridge (ed.), The blood-brain barrier. Raven Press, Ltd., New York, N.Y.
19. **Busso, M., J. Thornthwaite, and L. Resnick.** 1991. HIV-induced syncytium formation requires the formation of conjugates between virus-infected and uninfected T-cells in vitro. AIDS **5:**1425–1432.
20. **Büttner, A., P. Mehraein, and S. Weis.** 1996. Vascular changes in the cerebral cortex in HIV-1 infection. Acta Neuropathol. **92:**35–41.
21. **Elovaara, I., M. Iivanainen, S. L. Valle, J. Suni, T. Tervo, and J. Lahdevirta.** 1987. CSF protein and cellular profiles in various stages of HIV infection related to neurological manifestations. J. Neurol. Sci. **78:**331–342.
22. **Falangola, M. F., A. Hanly, B. Galvao-Castro, and C. K. Petito.** 1995. HIV infection of human choroid plexus: a possible mechanism of viral entry into the CNS. J. Neuropathol. Exp. Neurol. **54:**497–503.
23. **Filice, G., P. M. Cereda, and O. E. Varnier.** 1988. Infection in rabbits with human immunodeficiency virus. Nature **335:**366–369.
24. **Freed, E. O., and M. A. Martin.** 1995. The role of human immunodeficiency virus type 1 envelope glycoproteins in virus infection. J. Biol. Chem. **270:**23883–23886.
25. **Freed, E. O., and M. A. Martin.** 1995. Virion incorporation of envelope glycoproteins with long but not short cytoplasmi tails is blocked by specific, single amino acid substitutions in the human immunodeficiency virus type 1 matrix. J. Virol. **69:**1984–1989.
26. **Frost, E. H.** 1977. Radioactive labelling of viruses: an iodination preserving biological properties. J. Gen. Virol. **35:**181–185.
27. **Gendelman, H. E., J. Zheng, C. L. Coulter, A. Ghorpade, M. Che, M. Thylin, R. Rubocki, Y. Persidsky, F. Hahn, J. J. Reinhard, and S. Swindells.** 1998. Suppression of inflammatory neurotoxins by highly active antiretroviral therapy in human immunodeficiency virus-associated dementia. J. Infect. Dis. **178:**1000–1007.
28. **Gerhart, D. Z., M. A. Broderius, and L. R. Drewes.** 1988. Cultured human and canine endothelial cells from brain microvessels. Brain Res. Bull. **21:**785–793.
29. **Grossman, D. M., W. A. Banks, J. LeBlanc, and P. Dejace.** 1998. Prevalence of hypernatremia in HIV-infected VA patients. J. Investig. Med. **46:**46A.
30. **Gutierrez, E. G., W. A. Banks, and A. J. Kastin.** 1993. Murine tumor necrosis factor alpha is transported from blood to brain in the mouse. J. Neuroimmunol. **47:**169–176.
31. **Hall, C. D., C. R. Snyder, K. R. Robertson, J. A. Messenheimer, J. W. Wilkins, W. T. Robertson, R. A. Whaley, C. Van der Horst, and L. M. Silverman.** 1992. Cerebrospinal fluid analysis in human immunodeficiency virus infection. Ann. Clin. Lab. Sci. **22:**139–143.
32. **Hardebo, J. E., and J. Kahrstrom.** 1985. Endothelial negative surface charge areas and blood-brain barrier function. Acta Physiol. Scand. **125:**495–499.
33. **Harouse, J. M., Z. Wroblewska, M. A. Laughlin, W. F. Hickey, B. S. Schonwetter, and F. Gonzalez-Scarano.** 1989. Human choroid plexus cells can be latently infected with human immuodeficiency virus. Ann. Neurol. **25:**406–411.
34. **Harris, P. J. and R. Curry.** 1995. Diabetes insipidus and AIDS. J. Acquir. Immune Defic. Syndr. Hum. Retrovirol. **9:**99.
35. **Horan, P. J., A. Mattia, E. J. Bilsky, S. Weber, T. P. Davis, H. I. Yamamura, E. Malatynska, S. M. Appleyard, J. Slaninova, A. Misicka, A. W. Lipkowski, V. J. Hruby, and F. Porreca.** 1996. Antinociceptive profile of biphalin, a dimeric enkephalin analog. J. Pharmacol. Exp. Ther. **265:**1446–1454.
36. **Hurwitz, A. A., J. W. Berman, and W. D. Lyman.** 1994. The role of the blood-brain barrier in HIV infection of the central nervous system. Adv. Neuroimmunol. **4:**249–256.
37. **Johanson, C. E.** 1988. The choroid plexus-arachnoid membrane-cerebrospinal fluid system, p. 33–104. *In* A. A. Boulton, G. B. Baker, and W. Walz (ed.), Neuromethods; the neuronal microenvironment. The Humana Press, Clifton, N.J.
38. **Kage, A., E. Shoolian, K. Rokos, M. Ozel, R. Nuck, W. Reutter, E. Köttgen, and G. Pauli.** 1998. Epithelial uptake and transport of cell-free human immunodeficiency virus type 1 and gp120-coated microparticles. J. Virol. **72:**4231–4236.
39. **Koenig, H., J. J. Trout, A. D. Goldstone, and C. Y. Lu.** 1992. Capillary NMDA receptors regulate blood-brain barrier function and breakdown. Brain Res. **588:**297–303.
40. **Lafon, M. E., J. L. Gendrault, C. Royer, D. Jaeck, A. Kirn, and A. M. Steffan.** 1993. Human endothelial cells isolated from the hepatic sinusoids and the umbilical vein display a different permissiveness for HIV-1. Res. Virol. **144:**99–104.
41. **Lidinsky, W. A., and L. R. Drewes.** 1983. Characterization of the blood-brain barrier: protein composition of the capillary endothelial cell membrane. J. Neurochem. **41:**1341–1348.
42. **Maness, L. M., W. A. Banks, J. E. Zadina, and A. J. Kastin.** 1996. Periventricular penetration and disappearance of icv Tyr-MIF-1, DAMGO, tyrosine, and albumin. Peptides **17:**247–250.

43. **Marsh, M.** 1984. The entry of enveloped viruses into cells by endocytosis. Biochem. J. **218:**1–10.
44. **Miller, D. W.** 1999. Immunobiology of the blood-brain barrier. J. Neurovirol. **5:**570–578.
45. **Mondor, I., S. Ugolini, and Q. J. Sattentau.** 1998. Human immunodeficiency virus type 1 attachment to HeLa CD4 cells is CD4 independent and gp120 dependent and requires cell surface heparans. J. Virol. **72:**3623–3634.
46. **Montelaro, R. C., and R. R. Rueckert.** 1975. On the use of chloramine-T to iodinate specifically the surface proteins of intact enveloped viruses. J. Gen. Virol. **29:**127–131.
47. **Moses, A. V., F. E. Bloom, C. D. Pauza, and J. A. Nelson.** 1993. Human immunodeficiency virus infection of human brain capillary endothelial cells occurs via a CD4/galactosylceramide-independent mechanism. Proc. Natl. Acad. Sci. USA **90:**10474–10478.
48. **Moses, A. V., and J. A. Nelson.** 1994. HIV infection of human brain capillary endothelial cells-Implications for AIDS dementia. Adv. Neuroimmunol. **4:**239–247.
49. **Moses, A. V., S. G. Stenglein, J. G. Strussenberg, K. Wehrly, B. Chesebro, and J. A. Nelson.** 1996. Sequences regulating tropism of human immunodeficiency virus type 1 for brain capillary endothelial cells map to a unique region of the viral genome. J. Virol. **70:**3401–3406.
50. **Murakami, T., and E. O. Freed.** 2000. The long cytoplasmic tail of gp41 is required in a cell type-dependent manner for HIV-1 envelope glycoprotein incorporation into virions. Proc. Natl. Acad. Sci. USA **97:**343–348.
51. **Nottet, H. S., Y. Persidsky, V. G. Sasseville, A. N. Nukuna, P. Bock, Q. H. Zhai, L. R. Sharer, R. D. McComb, S. Swindells, C. Soderland, and H. E. Gendelman.** 1996. Mechanisms for the transendothelial migration of HIV-1-infected monocytes into brain. J. Immunol. **156:**1284–1295.
52. **Patlak, C. S., R. G. Blasberg, and J. D. Fenstermacher.** 1983. Graphical evaluation of blood-to-brain transfer constants from multiple-time uptake data. J. Cereb. Blood Flow Metab. **3:**1–7.
53. **Persidsky, Y., M. Stins, D. Way, M. H. Witte, M. Weinand, K. S. Kim, P. Bock, H. E. Gendelman, and M. Fiala.** 1997. A model for monocyte migration through the blood-brain barrier during HIV-1 encephalitis. J. Immunol. **158:**3499–3510.
54. **Pleskoff, O., N. Sol, B. Labrosse, and M. Alizon.** 1997. Human immunodeficiency virus strains differ in their ability to infect $CD4^+$ cells expressing the rat homolog of CXCR-4 (fusin). J. Virol. **71:**3259–3262.
55. **Poland, S. D., G. P. Rice, and G. A. Dekaban.** 1995. HIV-1 infection of human brain-derived microvascular endothelial cells in vitro. J. Acquir. Immune Defic. Syndr. Hum. Retrovirol. **8:**437–445.
56. **Power, C., P.-A. Kong, T. O. Crawford, S. Wesselingh, J. D. Glass, J. C. McArthur, and B. D. Trapp.** 1993. Cerebral white matter changes in acquired immunodeficiency syndrome dementia: alterations of the blood-brain barrier. Ann. Neurol. **34:**339–350.
57. **Preston, E., and I. Hynie.** 1991. Transfer constants for blood-brain barrier permeation of the neuroexcitatory shellfish toxin, domoic acid. Can. J. Neurol. Sci. **18:**39–44.
58. **Raub, T. J., and K. L. Audus.** 1990. Adsorptive endocytosis and membrane recycling by cultured primary bovine brain microvessel endothelial cell monolayers. J. Cell Sci. **97:**127–138.
59. **Resnick, L., J. R. Berger, P. Shapshak, and W. W. Tourtellotte**. 1988. Early penetration of the blood-brain-barrier by HIV. Neurology **38:**9–14.
60. **Triguero, D., J. Buciak, and W. M. Pardridge.** 1990. Capillary depletion method for quantification of blood-brain barrier transport of circulating peptides and plasma proteins. J. Neurochem. **54:**1882–1888.
61. **Villegas, J. C., and R. D. Broadwell.** 1993. Transcytosis of protein through the mammalian cerebral epithelium and endothelium. II. Adsorptive transcytosis of WGA-HRP and the blood-brain and brain-blood barriers. J. Neurocytol. **22:**67–80.
62. **Vorbrodt, A. W., D. H. Dobrogowska, M. Ueno, and A. S. Lossinsky.** 1995. Immunocytochemical studies of protamine-induced blood-brain barrier opening to endogenous albumin. Acta Neuropathol. (Berlin) **89:**491–499.
63. **Westergren, I., and B. B. Johansson.** 1993. Altering the blood-brain barrier in the rat by intracarotid infusion of polycations: a comparison between protamine, poly-L-lysine and poly-L-arginine. Acta Physiol. Scand. **149:**99–104.
64. **Wiley, C. A., R. D. Schrier, J. A. Nelson, P. W. Lampert, and M. B. A. Oldstone.** 1986. Cellular localization of human immunodeficiency virus infection within the brains of acquired immune deficiency syndrome patients. Proc. Natl. Acad. Sci. USA **83:**7089–7093.
65. **Willey, R. L., M. A. Martin, and K. W. C. Peden.** 1994. Increase in soluble CD4 binding to and CD4-induced dissociation of gp120 from virions correlates with infectivity of human immunodeficiency virus type 1. J. Virol. **68:**1029–1039.
66. **Winslow, B. J., and D. Trono.** 1993. The blocks to human immunodeficiency virus type 1 Tat and Rev functions inmouse cell lines are independent. J. Virol. **67:**2349–2354.
67. **Zambenedetti, P., R. Giordano, and P. Zatta.** 1996. Indentification of lectin binding sites in the rat brain. Glycoconj. J. **13:**341–346.
68. **Zatta, P. F., S. Zanoni, and M. Favarato.** 1994. Lectin histochemistry of the brain cortex in Alzheimer's disease, p. 141–153. *In* M. Nicolini and P. F. Zatta (ed.), Glycobiology and the brain. Pergamon Press, Oxford, England.
69. **Zhang, L., D. Looney, D. Taub, S. L. Chang, D. Way, M. H. Witte, M. C. Graves, and M. Fiala.** 1998. Cocaine opens the blood-brain barrier to HIV-1 invasion. J. Neurovirol. **4:**619–626.